The Iraqi Journal For Mechanical And Material Engineering, Vol.18, No.4, Dec, 2018

NUMERICAL AND EXPERIMENTAL INVESTIGATIONS OF CUTTING FORCE FOR NAB-CBN COMPOSITE

Alaa H. Jaafar Alaahus30@Gmail.com
Haydar Al-Ethari dralethariha h@yahoo.com

College of Materials Engineering / University of Babylon-Iraq

ABSTRACT

The alloy of nickel aluminum bronze (NAB) presents superior properties such as high strength, excellent wear resistance and corrosion resistance, so it's used in a wide range of engineering applications. Usually, this material undergo to a series of machining processes to achieve the final shape. In this paper, NAB alloy reinforced with cubic boron nitride (CBN) particles was fabricated by powder metallurgy route. Design of experiments has been used to study the effect of main turning parameters on the main cutting force for NAB-CBN composite. Numerical modelling was developed to predict the main cutting force required during turning process under different machining conditions. The results of numerical model showed that the maximum error comparing with the experiment results is not exceed 13.86%, which suggests that the developed model are reasonable. Optimization of machining process parameters was done using response surface method.

KEYWORDS: Numerical modelling, powder metallurgy, nickel aluminium bronze, design of experiments, main cutting force.

دراسة عددية وتجريبية لقوة القطع للمادة المركبة NAB-CBN

علاء حسين جعفر حيدر ألعذاري
جامعة بابل ـ العراق / كلية هندسة ألمواد

الخلاصة

سبيكة نيكل المنيوم برونز تظهر خواص متفوقه كمقاومة عالية، مقاومة بلى ومقاومة تآكل عالية, لذلك تستخدم بمدى واسع من التطبيقات الهندسية. دائما، تتعرض هذه المادة لمجموعه من عمليات التشغيل للحصول على الشكل النهائي. في هذا البحث، تم تصنيع سبيكة نيكل المنيوم برونز مقواة بدقائق من نتريد البورون ذي التركيب المكعب بطريقه ميتالورجيا المساحيق .تم استخدام تصميم التجارب لدراسة تأثير ألمتغيرات الرئيسية لعملية الخراطة على قوة القطع الرئيسية للمادة المركبة NAB-CBN. تم تطوير نمذجة عددية للتنبوء بقوة القطع الرئيسيه المطلوبة خلال عملية ألخراطة تحت ظروف تشغيل مختلفة. أظهرت النتائج بان اعلى نسبة خطأ للنموذج العددي المطور هو 13.86%، وهذا يوحي بان النموذج العددي المطور هو نماذج منطقية. تم اجراء الامثلية لمتغيرات عملية التشغيل بأستخدام اسلوب تاجوشي.

Received: 2017 - 12 - 11
Accepted: 2018 - 1 - 15

INTRODUCTION:-

Nickel-aluminium bronze (NAB) is a series of copper-based alloy with additions of aluminium, nickel, and iron. This alloy shows a good combination of properties such as high strength, good resistance to corrosion and wear, which makes it one of the most versatile engineering materials that can be used as seawater valve, piping systems, seawater external hatches, sonar equipment, fasteners and sealing flanges, hydraulic valves and bearings [Prabhash Jain et.al., 2013]. Copper with (8-11% Al) consist of α (Cu) phase and a second phase appears at high temperature known as β phase, β phase becomes unstable during cooling and decomposes to α phase and γ2 (Al4Cu9) phase which is not desirable [Daroonparvar M.R. et.al., 2011]. Addition of nickel and iron to copper-aluminium alloys increase its mechanical properties through the precipitation of several κ phases (NiAl and Fe3Al) among α and β phases. NAB alloys are characterized by their excellent corrosion behaviour, partially because Ni and Fe extend the terminal α phase field and suppress the γ2 phase formation that occurs in binary Cu-Al alloys [Ivan Richardson et.al., 2016]. In the manufacturing process of some important industrial and marine pieces of NAB alloy such as screw propeller, thin pieces are cooled by high rate and parting is developed because of more changes in rate of cooling in different pieces and in the result, it leads to porous damages. Given problems lead to decreasing hardness and strength of this alloy. The hardening of NAB alloy is required to increase the age of the pieces produced by NAB alloy [Keshavarz el.al., 2016]. In this regard, few works had been published. Haydar and Hussain (2014) studied the effect of SIC and graphite as reinforcement element on physical, mechanical, and machining properties of NAB alloy prepared by powder metallurgy, Keshavarz and Abbasi, (2016) studied the improvement of the surface structure of NAB alloy by adding Al_2O_3 nanoparticles using friction stir process (FSP) method, Abbasi and Keshavarz, (2017) studied the corrosion properties and microstructure of NAB/Al_2O_3 surface nano composite. In the present work, cubic boron nitride (CBN) is used as reinforcement due to its unique combination of properties, such as very high hardness, low density, high melting point, high thermal conductivity and high electrical resistivity [Sankaranarayanan Seetharaman el.al., 2013]. Nickel aluminium bronze alloy reinforced with ceramic particles is more difficult to machine than typical bronze and this bring forward to investigate its machining properties [Medicus K. M. el.al., 2001].

The numerical models based on the Finite Element Method (FEM) helps the designer to design and optimize the production process in order to understand the best operative parameters and avoid expensive experimental campaigns [Arrazola P.J. et.al., 2013]. To understand the influence of machining conditions and to predict cutting forces for NAB based composite, specialized software DEFORM 2D was used to simulate orthogonal cutting. The software uses the finite element method for modelling the dynamics of pure plastic or elastic-plastic deformation processes. In DEFORM 2D simulation both tool and workpiece can be defined in the software. The incremental movement of the active part of the cutting tool is simulated and, if necessary, the software remodels the mesh automatically and calculations are continued.

This study aims at improving the mechanical properties of NAB fabricated via powder metallurgy route by reinforcing it with CBN particles. The specimen with the best percentage of reinforcement content (based on hardness) will be relied in this study. Experimental and numerical machining processes will be done to investigate the effect of machining conditions on the main cutting force of this specimen

EXPERIMENTAL DETAILS:-

The Powders of copper, aluminium, nickel, iron and cubic boron nitride were supplied from Lemandou Ltd. co. China. X-Ray Florescence (XRF) analysis for the used powders was carried

out using XRF analyzer type (Ds-2000) at General Company for Inspection and Engineering Rehabilitation-Baghdad. Particle size analysis was carried out by using laser particle size analyzer type (Bettersize 2000) at the University of Babylon/College of Materials Eng. /Ceramics and Building Materials Labs. The results of XRF test and the averages of particle size for the used powders are shown in Table 1.

Nickel aluminium bronze alloy with chemical composition of (Cu-9%Al-5%Ni-4%Fe) according to ASTM B150 [Ivan Richardson et.al., 2016] was prepared by powder metallurgy (PM), samples with (0, 0.5, 1, 1.5, and 2wt %) of CBN particles as a reinforcing element were prepared. A wet mixing was used with 2%wt of acetone. A mixing process for 6 hours was achieved by an electrical mixer type (STGQM-15⁄-2). Uniaxial compacting via double action steel die was carried out on electro hydraulic compacting machine type (Channel automatic cube and cylinder compression machines, CT340- CT440, USA). Lubricant was used for the inside walls of the die.

Three types of samples were prepared. Cylindrical samples with (19mm) in diameter and (12mm) in height used for hardness, X-Ray diffraction, thermal conductivity, chemical composition analysis and machining tests; samples with a diameter of (9mm) and a height of (13.5mm) was used for compression test according to ASTM B925–08 specifications [Haydar A. H. Al-Ethari et.al., 2014]; and samples with 10mm in diameter and 50mm in height used for coefficient of thermal expansion test and ultrasonic wave tests according to ASTM E494 - 95 [Mohammad Hamidnia et.al., 2012].

The preferred compacting pressure was determined experimentally based on the pressure that gives the highest green density. Green density increases with increasing the compacting pressure until it reaches a maximum effect in (700MPa) then slight increase on green density was observed when the pressure exceeds this value, so a compacting pressure of (700MPa) was used to prepare all samples. The sintering process of the green compact samples was achieved via vacuum high temperature tube furnace with a pressure of 10^{-4} torr. The sintering program is shown in Figure(1). The samples were left inside the furnace to cool down to room temperature. A heat treatment for the sintered samples was carried out by heating to a temperature of (900°C) for (50min) with a heating rate of (10°C/min), then quenching in cold water and tempered at (500°C) for (30min). Chemical composition analysis was carried out for the heat treated NAB alloy using metal analyser of model SPECTROMAXx at General Company for Inspection and Engineering Rehabilitation-Baghdad. The results are shown in Table 2.

X-Ray Diffraction (XRD) analysis was carried out via (MiniFlex 2) to the heat treated NAB alloy to insure the formation of desired phases. The analysis had been done at General Company for Inspection and Engineering Rehabilitation-Baghdad. The testing conditions are: (Target: Cu, wave length of 1.54060A°, voltage and current are 30 KV and 15 mA respectively, scanning speed (2deg/min.), and scanning range of (20^{o}-90^{o})). Micro-Vickers hardness test was done to all prepared samples to study the effect of CBN addition on the hardness. Appropriate grinding and polishing were carried out before subjecting the specimens to the test. The test was conducted at micro Vickers hardness device type (Digital Micro Vickers Hardness Tester TH 717) using a load of 500g for 10sec with a square-base diamond pyramid. The hardness was recorded as an average of five readings for each specimen.

Compression test, thermal conductivity test, thermal expansion test and ultrasonic wave test was carried out to the specimen with the preferred mechanical properties (based on hardness) to represent its behavior during simulation process through DEFORM 2d software. Compression test was conducted at universal testing machine type (Computer control electronic universal testing machine, model WDW-200 max load capacity 200KN) with a piston speed of 0.2 mm/min. the Thermal conductivity test was done by using thermal coefficient meter of type: YBF-3. Thermal expansion was tested by using Thermo-mechanical analysis instrument of type Quickline-05. Ultrasonic wave test was done to measure the elastic properties using Ultrasonic

wave device of type: cct-4 was used and digital monitor appears directly the time of transferred of ultrasonic wave. Elastic modulus and Poisson's ratio can obtain by applying the longitudinal and transverse velocities value on equations 1 and 2 [Santhosh Kumar S. *et.al.*, 2009].

$$\nu = (1 - 2\left(\frac{V_T}{V_L}\right)^2)/(2 - 2\left(\frac{V_T}{V_L}\right)^2) \quad (1)$$

$$E = V_L^2\, \rho\, (1+\sigma)(1-2\sigma) \,/\, (1-\sigma) \quad (2)$$

Where: ν: Poisson's ratio, V_T: Shear (Transverse) velocity (m/sec), V_L: Longitudinal velocity $(m/sec.)$, E: Elastic modulus (GPa), ρ: Density (Kg/m^3).

Design of Machining Experiments

The sample with preferred mechanical properties was prepared for the face turning machining. The sample was machined according to a program designed via Taguchi method L16 (4^3) orthogonal array to reduce the number of experiments and analysis the effect of machining conditions (namely cutting speed, feed rate and depth of cut) on the main cutting force using analysis of variance (ANOVA). The turning process was carried out at University of Babylon /College of Engineering/Mechanical Labs. All experiments were conducted in a lathe machine of type Harrison-m300 with spindle speeds of 58-2500 rpm and feed rates of 0.03-1 mm/rev. Table 3 demonstrates the controlled factors, designation, and levels.

The machining experiments were carried out under dry conditions by using Tungsten carbide tool with nose radius of 1.6mm and a tool angle of 55°. The chemical composition of the tool is (65 wt% W; 9 wt% Co, 26 wt% (TaC + TiC)). A new tool tip was used for every machining process. During each machining process the cutting forces were recorded using cutting force dynamometer of type: (IEICOS -Model 620B:200 Kgf), mounted on the lathe machine and connected to a charge amplifier of type: (IEICOS-Model 652) to display the force.

Finite Element Set Up

The finite element model used for orthogonal machining simulation was based on the lagrangian implicit code of the commercial finite element analysis (FEA) software DEFORM-2D (version 9). The plane strain assumption was utilized, the workpiece modelled as elasto-plastic with 1mm width and 3mm length body and initially meshed with 2000 elements. An uncoated tungsten carbide (WC) tool modelled as rigid body due to high elastic modulus of the cutting tool relative to the workpiece material, the tool meshed with 1000 elements. A high mesh density was defined at the upper part of the workpiece and at the tip of the tool (deformation zone) as shown in Figure(2) to obtain accurate chip formation process. The flow behaviour, elastic and thermal properties of the workpiece were provided from the experimental results, while tungsten carbide defined from the library of materials found in DEFORM-2D software.

The cutting processes were done at ambient temperature (20 ℃) with various cutting speed, feed rate, and depth of cut. All processes were carried out at constant rake angle of -5° and clearance angle of +5°, a heat transfer coefficient of 45 N/sec/mm/°C and no coolant was set. In this study, the shear friction factor modified to 0.3 and has been relied in all simulation processes based on earlier work [İrfan and Kubilay, 2011], because the forces data are sufficiently reliable and less sensitive over a wide range of frictional values as indicated in previous work [Filice, L.F. et al., 2007]. The workpiece was constrained in all directions while the tool was fixed in the vertical direction and was allowed to move horizontally. The machining process was eventually produced by applying a horizontal displacement boundary condition on the tool.

When the elements in the vicinity of the tool tip are highly distorted during the cutting simulation, the re-meshing procedure starts and a new mesh is generated. At this stage, the

solution information from the old mesh (stresses, strains, strain rates, and temperatures) is interpolated onto the new mesh and then the simulation continues. As a result, the chip is progressively separated from the workpiece and continues to flow over the rake face of the cutting tool. During this period of simulation, the cutting forces and temperature at the tool-chip interface increase progressively till steady state process is reached. After completing the simulation process, main cutting force were extracted from the postprocessor module in the software.

RESULTS AND DISCUSSION

Figure(3) demonstrates the XRD analysis for the heat treated NAB alloy. The diffraction patterns indicated the formation of κ phases due to the presence of iron and nickel, as well as the presence of α (Cu) phase, and this prove that the sintering of alloy for 90min at 930°C followed by heat treatment assists to get microstructure with solid solution alloy α phase and κ phases. The results are in good agreement with the reference [Yuting Lv el.al., 2015].
The results of micro-hardness test are shown in Figure(4). The results show a significant increase in hardness due to the heat treatment of the samples, these confirm the formation of martensitic phase which is very hard. The hardness of the NAB are in agreement with previous works [Ashkan Vakilipour Takaloo et.al., 2011, Keshavarz el.al., 2016]. With increasing in percentage of CBN the hardness increases significantly, this increment could be attributed to the very high hardness of CBN particles which is tend to restrain movement of the matrix and act as barriers to dislocation motion, so the hardness increases. With a percentage of CBN more than 1.5% the improvement in hardness is unremarkable, so this percentage was relied in this study, i.e. all tests will be based on this sample.
The compression test for NAB-1.5CBN composite recorded a compressive strength of 558 MPa, which are obtained from the stress – strain diagram shown in Figure(5). The stress strain curve of compression test was used to represent the behaviour of plastic deformation of NAB-1.5CBN composite as was used in earlier work [Guo Y.B., 2003] at constant strain rate of (0.015) and constant temperature (20℃).
The thermal conductivity and coefficient of thermal expansion for NAB-1.5CBN sample were 36 W/m.°c and 15.1 (10^{-6}/℃) respectively. The elastic modulus and poisons ratio were obtained as 131 GPa and 0.31 respectively. These results were used to represent the behavior of elastic and thermal properties of the composite in the simulation process.

Experimental Machining Results

The experimental results based the experimental design, created by all possible combinations of machining parameters (namely the cutting speed, feed rate, and depth of cut), is recorded in Table 4. Analysis of variance (ANOVA) was applied to investigate the effect of machining conditions on main cutting force and percentage of contribution of that effect as shown in Table 5. Main effect plots was used to indicate the effect of cutting speed, feed rate, and depth of cut on the main cutting force as shown in Figure(6)..
The analysis shows a small effect of cutting speed on the main cutting force compared with the feed rate and depth of cut. The analysis of the effect of cutting speed on main cutting force shows a slight decreasing in the main cutting force with increasing cutting speed because the formation of the high temperature which lead to thermal softening of workpiece and then the forces decreases gradually.
The feed rate has the largest effect on the main cutting force as shown in the analysis, the main cutting force increases significantly with increasing feed rate. Increasing the feed rate, the section of sheared chips is increasing and consequentially the removal of material requires higher forces. Chip cross-sectional area increases with the increase of feed rate, so it causes increase in

the amount of deviation of the curve. The main cutting force increase with increasing in the depth of cut, large quantity of workpiece was eliminated when the depth of cut was raised, so the plastic deformation was increased and this in turn raises the required force. These results are in agreement with reference [Sivaramana, V., et.al., 2012].

Numerical Machining Results

The process parameters have been defined according to orthogonal array (L16) which includes 16 runs of simulations. The properties of the workpiece material were obtained by experimental results. The flow stress behavior of the workpiece material was represented by the stress - strain curve that obtained from the compression test. A comparison between the simulation and experimental results for the main cutting force is shown in Table 6, scatter plot and main effect plot are shown in Figure(7) and Figure(8) respectively. ANOVA was done to the simulation results (shown in Table 7) to estimate the contribution percentage of machining conditions on the main cutting force. Figure(9) shows a simulation process at different steps

The results show an error range of 3.25%-13.86% between the simulation results of main cutting force and experimental main cutting force results. According to the ANOVA results, the machining conditions of the simulation and experimental processes have the same effect on the main cutting force but with different contribution percentage. The simulated main cutting force increases with the increase feed rate due to the increase in the section of sheared chips, and higher force is required to remove the metal. The increase in depth of cut was also observed to increase the main cutting force in the simulation process, and this is due to increase the volume of workpiece need to be cut and consequentially plastic deformation rises which is required high forces. The simulated main cutting force was found to be decreased with the increase of cutting speed due to the thermal softening.

The simulation processes was observed to have higher sensitive to the feed rate compared with experimental processes. In addition, the contribution percentage of depth of cut is low in simulation results compared with experimental results. These differences rises the error percentage when the feed rate has high values. However, the error percentages are within an acceptable limit and the model can be performed successfully to predict the cutting force during the machining process. The rapprochement between the cutting forces, resulted from the simulation and experiment, insures the accuracy of experimental results.

The simulation of machining processes by FEM showed great advantages, the analysis solved contact problems between bodies with complex properties of the workpiece and that’s can provide great benefits especially when orthogonal cutting is a common process in industry. Creating accurate models using FEM can help in optimizing these processes, reduction of the experiments number and reduction in time and costs. In addition, many output data can be obtained such as strain, stress, deformation, surface roughness, temperature and tools wear.

Optimization Results

Response surface method was utilized in this study to set the optimal parameters that can be used to minimize the main cutting force during cutting NAB-1.5CBN composite. The optimal set of lathe parameters are: cutting speed as 3.46 m/min, depth of cut as 0.25 mm and feed rate as 0.05 mm. These parameters can provide a face turning process to such composite with 40.9N main cutting force. In order to verify the predicted results, a confirmation of the optimum results was done by applying optimum machining conditions experimentally and the results is shown in Table 8. The error percentage found within permissible limits.

CONCLUSIONS:-

According to the results of the present work, the following can be concluded:
1. Cubic boron nitride with 1.5% percentage can serve effectively as reinforcement in nickel aluminium bronze alloy.
2. The main cutting force is highly dependent on feed rate followed by depth of cut, a slight effect of cutting speed was observed during machining NAB-CBN composite.
3. The developed numerical model can predict the main cutting force in the machining of NAB-CBN composite with acceptable error range.

ACKNOWLEDGMENT

The authors wish to acknowledge entire staff of materials engineering college and engineering college/University of Babylon-Iraq for their extended help during fabrication and experimentation activities.

Table 1: The purity and the average particle size of the powders used

Powder	Purity	Average Particles Size (µm)
Copper	99.10	1.171
Aluminium	99.35	2.341
Nickel	99.27	1.922
Iron	98.70	5.062
Boron Nitride	99.50	0.42

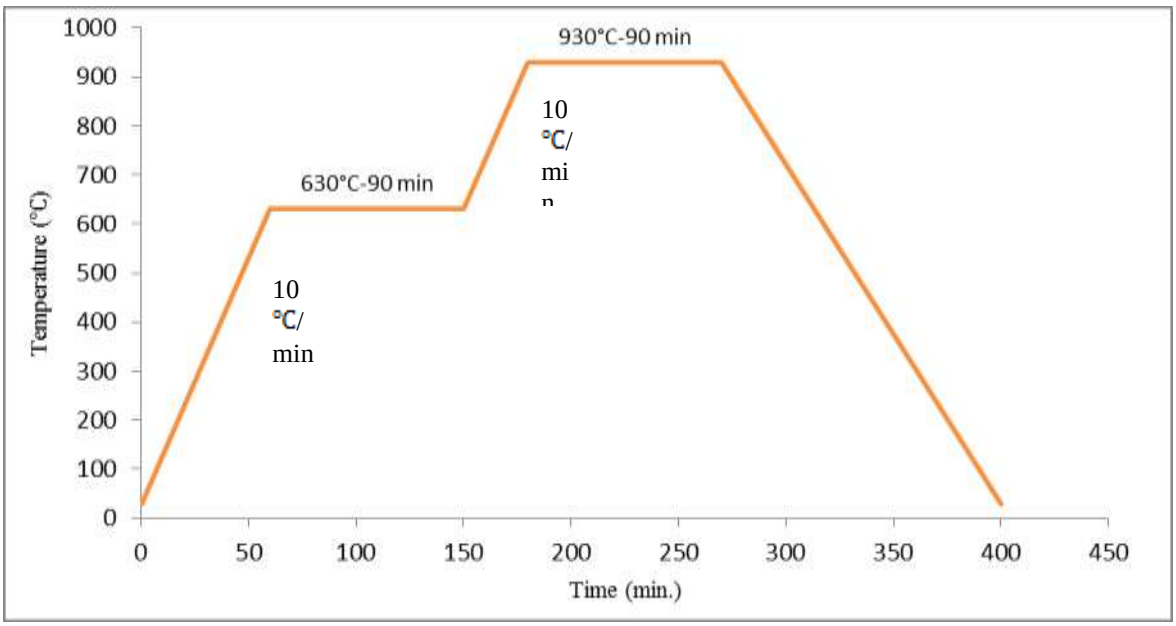

Fig. 1: The Sintering Program of the Green Samples

Table 2: Chemical Composition of Prepared Samples

Weight percentage of the elements (%)			
Cu	Al	Ni	Fe
81.7	8.8	5.1	3.48

Table 3: Control Factors and their Levels

Parameter	Designation	Unit	Levels			
			1	2	3	4
Cutting Speed	V_c	m/min	3.46	10.73	15.5	22
Feed Rate	f	mm/rev.	0.05	0.1	0.16	0.2
Depth of Cut	d	mm	0.25	0.5	0.75	1

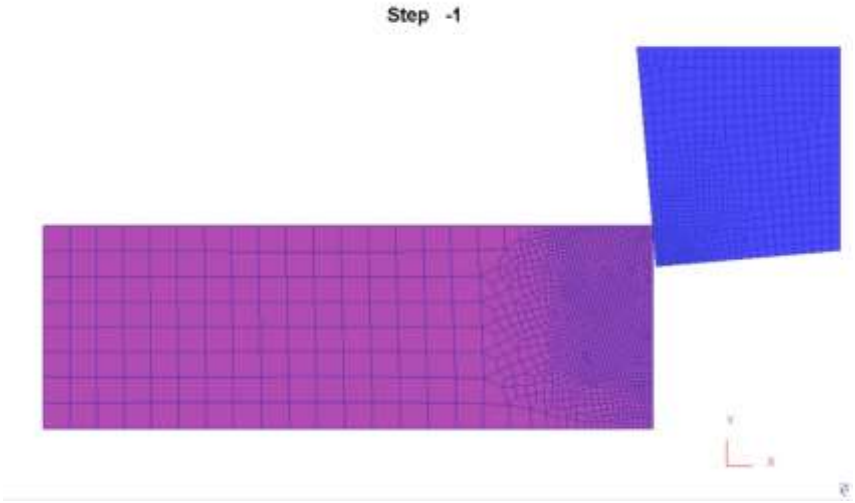

Fig. 2: Designed tool and workpiece and their meshes

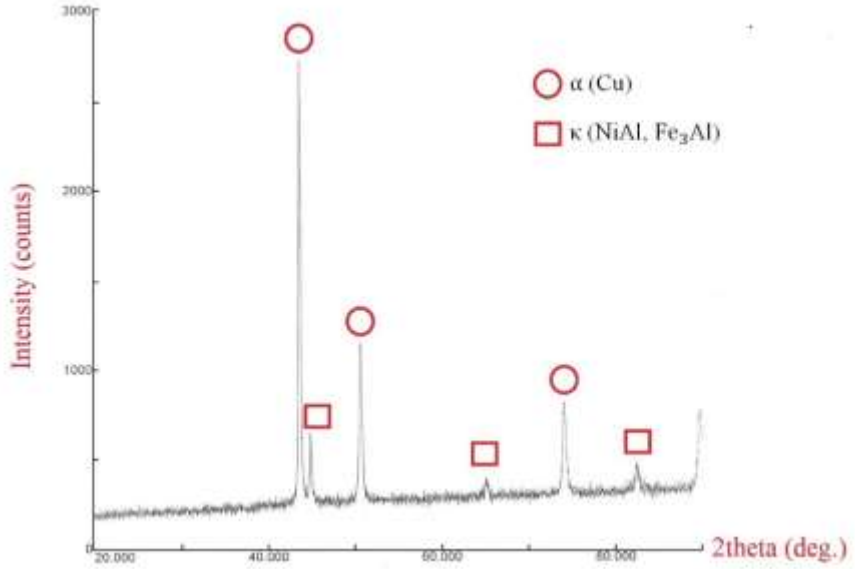

Fig. 3: XRD Pattern of Heat Treated NAB Alloy

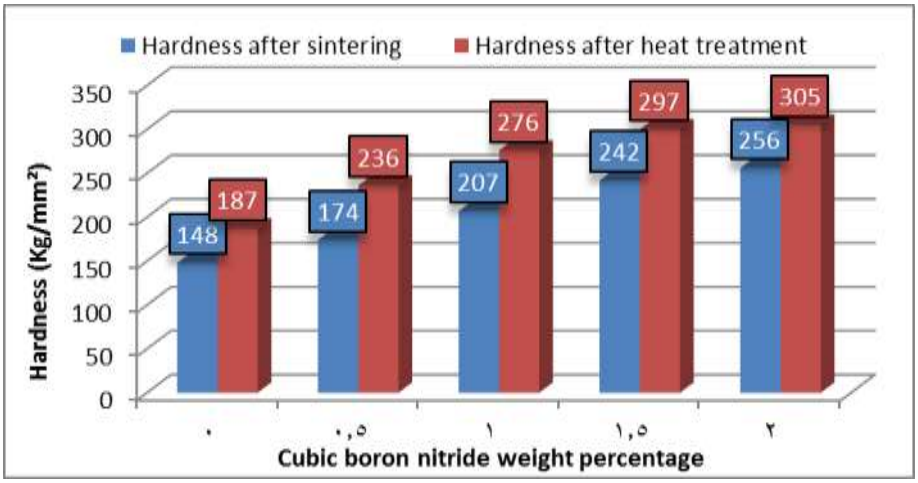

Fig. 4: Vickers hardness results of the prepared samples

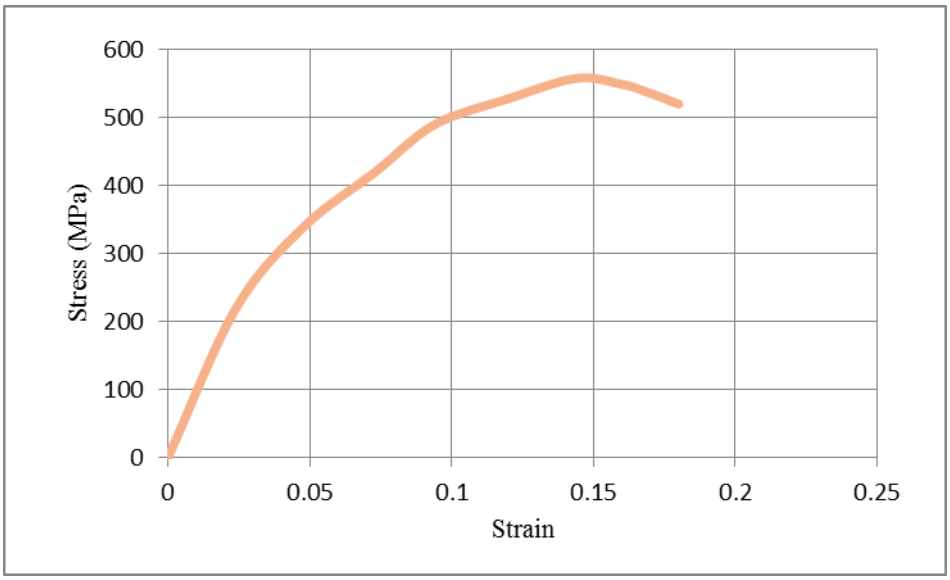

Fig. 5: Stress-Strain Curve of NAB-1.5%CBN Sample

Table 4: Experimental results of main cutting force

NO.	Cutting speed (m/min)	Feed rate (mm/rev.)	Depth of cut (mm)	Main cutting force (N)
1	3.46	0.05	0.25	39.28
2	3.46	0.10	0.50	88.38
3	3.46	0.16	0.75	137.48
4	3.46	0.20	1.00	186.58
5	10.73	0.05	0.50	49.10
6	10.73	0.10	0.25	78.56
7	10.73	0.16	1.00	147.30
8	10.73	0.20	0.75	157.12
9	15.50	0.05	0.75	58.92
10	15.50	0.10	1.00	117.84
11	15.50	0.16	0.25	98.20
12	15.50	0.20	0.50	117.84
13	22.00	0.05	1.00	68.74
14	22.00	0.10	0.75	78.56
15	22.00	0.16	0.50	108.02
16	22.00	0.20	0.25	108.02

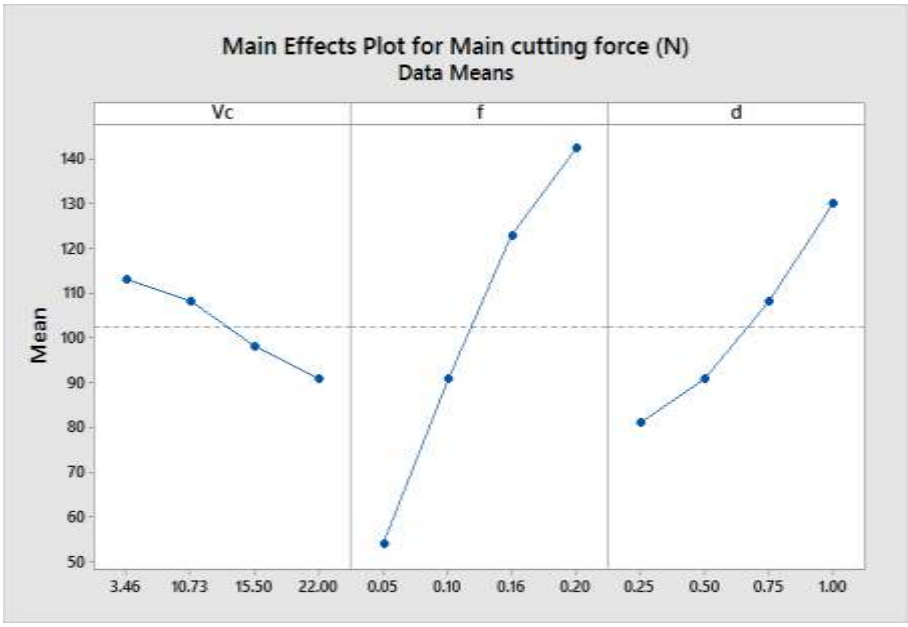

Fig. 6: Main effect plot for means of main cutting force

Table 4: ANOVA results for experimented main cutting force

Main Cutting Force Versus Cutting Speed					
Source	DF	SS	MS	F-value	p-value
V_c	3	1175	391.8	0.2	0.897
Error	12	23891	1990.9		
Total	15	25066			
Main Cutting Force Versus Feed Rate					
Source	DF	SS	MS	F-value	p-value
f	3	17955	5984.8	10.10	0.001
Error	12	7112	592.7		
Total	15	25066			
Main Cutting Force Versus Depth of Cut					
Source	DF	SS	MS	F-value	p-value
d	3	5563	1854	1.14	0.372
Error	12	19503	1625		
Total	15	25066			
Percentage of Contribution					
V_c = 4.69		f = 71.63		d = 22.19	

Table 5: Simulation and experimented results of main cutting force

NO.	Cutting speed (m/min)	Feed rate (mm/rev.)	Depth of cut (mm)	Main cutting force (N)		Error %
				Exp.	simu.	
1	3.46	0.05	0.25	39.28	43	9.47
2	3.46	0.10	0.50	88.38	95	7.47
3	3.46	0.16	0.75	137.48	150	9.10
4	3.46	0.20	1.00	186.58	210	12.55
5	10.73	0.05	0.50	49.10	53	7.94
6	10.73	0.10	0.25	78.56	87	10.74
7	10.73	0.16	1.00	147.30	156	5.90
8	10.73	0.20	0.75	157.12	173	10.10
9	15.50	0.05	0.75	58.92	57	3.25
10	15.50	0.10	1.00	117.84	110	6.65
11	15.50	0.16	0.25	98.20	111	13.00
12	15.50	0.20	0.50	117.84	133	12.86
13	22.00	0.05	1.00	68.74	64	6.89
14	22.00	0.10	0.75	78.56	86	9.47
15	22.00	0.16	0.50	108.02	117	8.30
16	22.00	0.20	0.25	108.02	123	13.86

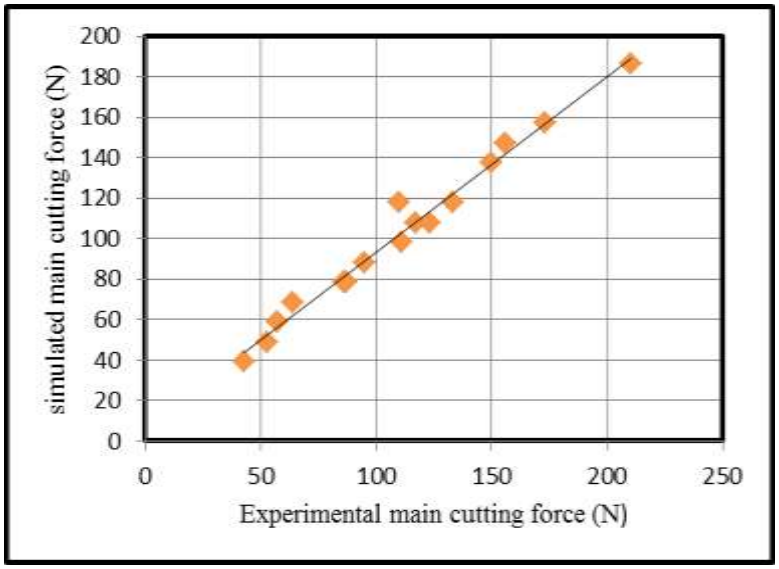

Fig. 7: Scatter plot of simulated and experimented main cutting force

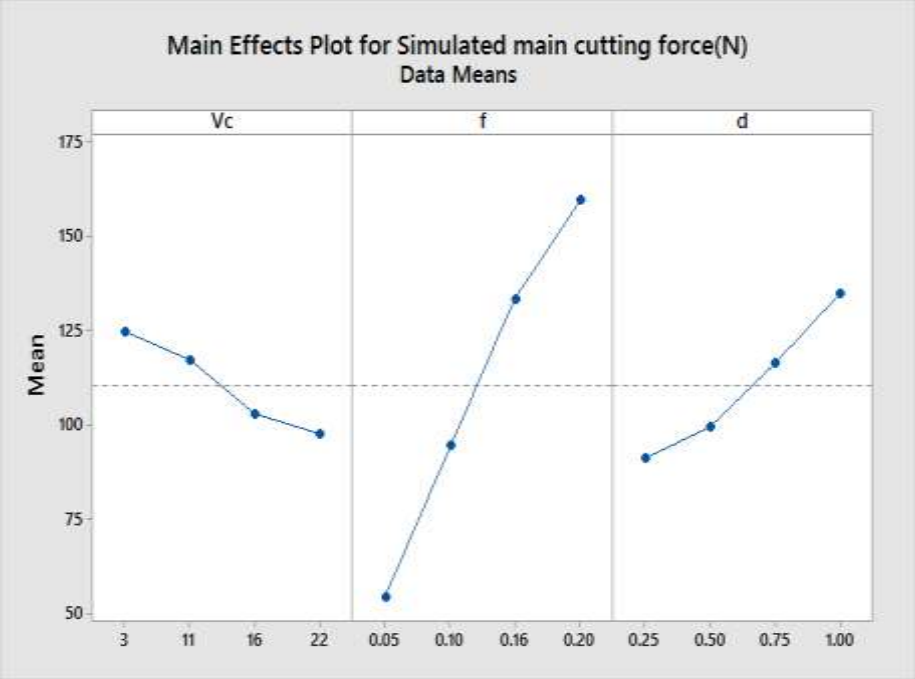

Fig. 8: Main effect plot for means of simulated main cutting force

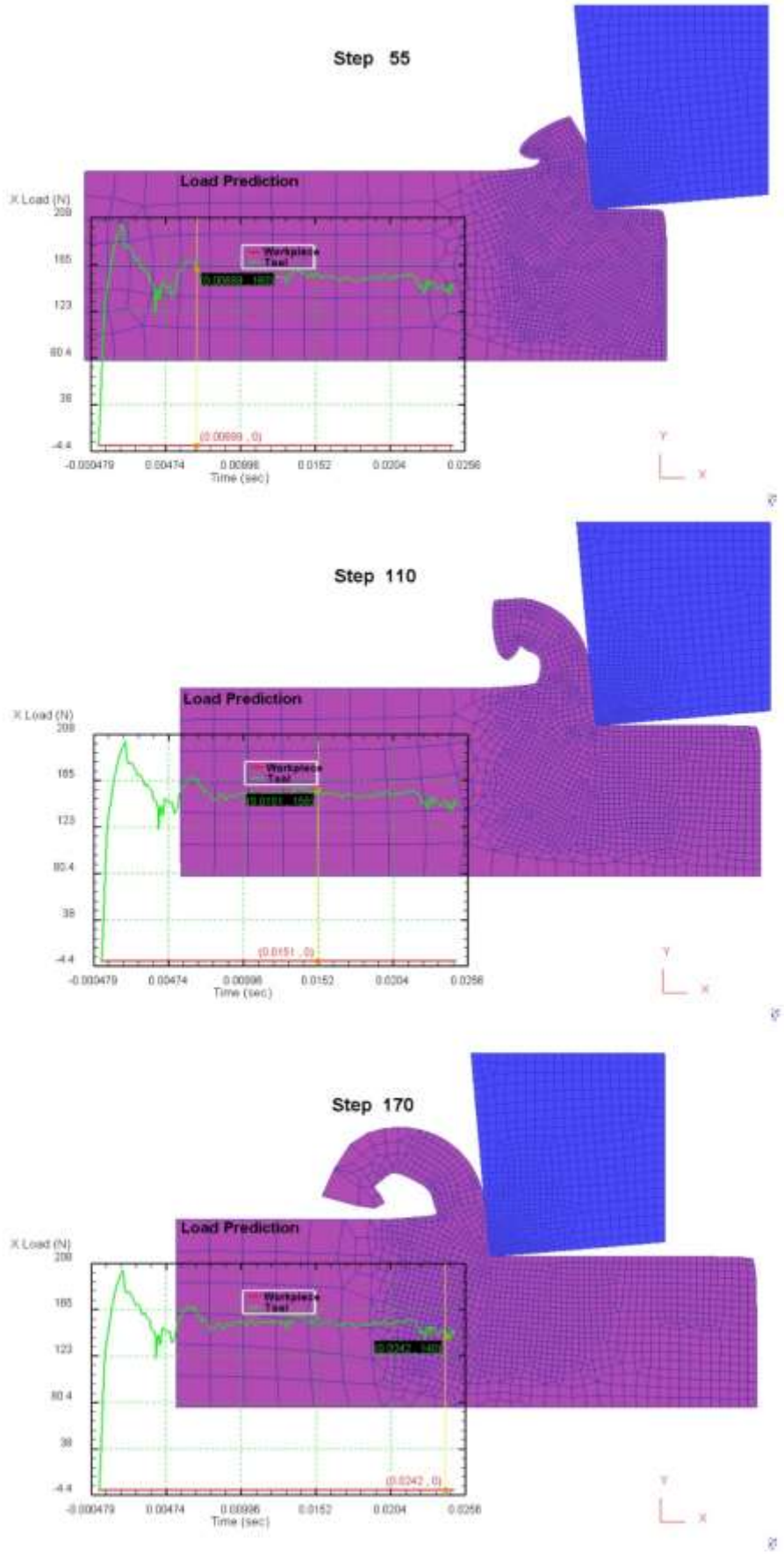

Fig. 9: Simulation steps at V=3.46, f=0.16, d=0.75

Table 6: ANOVA results for simulated main cutting force

Main Cutting Force Versus Cutting Speed					
Source	DF	SS	MS	F-value	p-value
S	3	1882	627.5	0.25	0.862
Total	12	30539	2545.0		
Error	15	32422			
Main Cutting Force Versus Feed Rate					
Source	DF	SS	MS	F-value	p-value
f	3	25499	8499.5	14.73	0.000
Total	12	6923	577.0		
Error	15	32422			
Main Cutting Force Versus Depth of Cut					
Source	DF	SS	MS	F-value	p-value
d	3	4550	1517	0.65	0.596
Total	12	27872	2323		
Error	15	32422			
Percentage of Contribution					
V_c = 5.81		f = 78.65		d = 14.03	

Table 7: Confirmation Results

Parameter	Experimental	Predicted	Error %
Main cutting force (N)	40.9	39.2	4.3

REFERENCES:-

Abbasi Khazaei, and Keshavarz. 2017. Nickelaluminum-bronze/Al_2O_3 surface nanocomposite produced by friction-stir processing: Corrosion properties and microstructure. Materials and Corrosion. 68: 883-891

Arrazola P.J., Özel T., Umbrello D., Davies M., Jawahir I.S. (2013), Recent advances in modelling of metal machining processes, CIRP AnnalsManufacturing Technology 62:695–718.

+Ashkan Vakilipour Takaloo, Mohammad Reza Daroonparvar, Mehdi Mazar Atabaki, and Kamran Mokhtar (2011) 'Corrosion Behavior of Heat Treated Nickel-Aluminum Bronze Alloy in Artificial', Materials Sciences and Seawater Applications, Vol. 2, No. 11, pp. 1542-1555.

Daroonparvar M.R., Mazar Atabaki M., Vakilipour A. "Effect Of Pre-Heat Treatment On Corrosion Behavior Of Nickel-Aluminium Bronze Alloy", Association of Metallurgical Engineers of Serbia, Vol. 17, p.p. 183-198, 2011.

Filice, L.F. Micari, F. Rizzuti, S. and Umbrello, D. (2007) 'A critical analysis on the friction modelling in orthogonal machining', International Journal of Machine Tools & Manufacture, Vol. 47, pp. 709-714.

Guo Y.B., (2003) 'An integral method to determine the mechanical behaviour of materials in metal cutting', Journal of Materials Processing Technology, Vol. 142, p.p. 72-81.

Haydar A. H. Al-Ethari, Ali Hobi Haleem, Hala Hazim Aiqaissy (2014) 'Effect Of Graphite On Mechanical And Machining Properties Of Al-Bronze Prepared By P/M', International Journal of Mechanical Engineering and Technology, Vol. 5, No. 5, pp. 189-199.

Haydar A. H. Al-Ethari and Hussain Hamza. 2014. Tool Life Modeling for Drilling NAB Alloy Reinforced by SIC and Graphite. IJEIT. 3(7):13-17

İrfan Ucun and Kubilay Aslantas (2011) 'Numerical simulation of orthogonal machining process using multilayer and single-layer coated tools', The International Journal of Advanced Manufacturing Technology, Vol. 54, pp.899-910.

Ivan Richardson, Carol Powell "Guide to Nickel Aluminium Bronze for Engineers" Copper Development Association Publication, No 222, 2016.

Keshavarz and Abbasi Khazayi (2016) "Improvement the surface structure of Nickel-Aluminum Bronze (NAB) alloy using Al2O3 nanoparticles and FSP method", American Journal of Oil and Chemical Technologies, Vol. 4, p.p. 4-13.

Medicus K. M., M. A. Davies, B. S. Dutterer, C. J. Evans, and R. S. Fielder (2001) "Tool Wear And Surface Finish In High Speed Milling Of Aluminum Bronze", Machining Science And Technology, Vol. 5, p.p. 255-268.

Mohammad Hamidnia and Farhang Honarvar. (2012) 'Measurement Of Elastic Properties Of Aisi 52100 Alloy Steel By Ultrasonic Nondestructive Methods', Journal Of Mechanics Of Materials And Structures, Vol. 7, No. 10, pp. 951-961.

Prabhash Jain, and Praveen Kumar Nigam, (2013) "Influence of Heat Treatment on Microstructure and Hardness of Nickel Aluminium Bronze (Cu-10al-5ni-5fe)", IOSR Journal of Mechanical and Civil Engineering, Vol. 4, p.p. 16-21.

Sankaranarayanan Seetharaman , Jayalakshmi Subramanian , Khin Sandar Tun , Abdelmagid S. Hamouda, and Manoj Gupta, (2013) "Synthesis and Characterization of Nano Boron Nitride Reinforced Magnesium Composites Produced by the Microwave Sintering Method", materials, Vol. 6, p.p. 1940-1955.

Santhosh Kumar, Seshu Bai V., Rajkumar G. K. Sharma, Jayakumar T., and Rajasekharan1 T. (2009) 'Elastic modulus of Al–Si/SiC metal matrix composites as a function of volume fraction', Journal of Physics D: Applied Physics, Vol. 42 No. 17, pp. 1-10

Sivaramana V.. Sankaran S., Vijayaraghavan L., (2012) 'The Effect of Cutting Parameters on Cutting Force During Turning Multiphase Microalloyed Steel', Procedia CIRP, Vol. 4, pp. 157 – 160.

Yuting Lv, Liqiang Wang , Xiaoyan Xu and Weijie Lu (2015) 'Effect of Post Heat Treatment on the Microstructure and Microhardness of Friction Stir Processed NiAl Bronze (NAB) Alloy', Metals, Vol. 5, No. 3, pp. 1695-1703.